

# Adaptive Subcarrier Block Modulation with Differentially Modulated Pilot Symbol Assistance for Downlink OFDM Using Uplink Delay Spread

Chang-Jun AHN<sup>†a)</sup>, Satoshi TAKAHASHI<sup>†\*</sup>, Hiroshi HARADA<sup>†</sup>, Yukiyo KAMIO<sup>†</sup>,  
and Iwao SASASE<sup>††</sup>, *Members*

**SUMMARY** In AMS/OFDM systems, base station is in control of the modulation level of each subcarrier, and then, adaptive modulated packet is transmitted from the base station to the mobile station. In this case, the mobile station is required the modulation level information (MLI) to demodulate the received packet. The MLI is generally transmitted as a data symbol, therefore, the throughput is degraded. In an OFDM, the channel response at a particular subcarrier frequency is not supposed to be totally different from its neighboring frequencies, and hence, they must have correlation which depends on the coherence bandwidth of the channel  $B_c$ . If we could assign the same modulation level for coherently faded subcarrier block, MLI is required only one time for each subcarrier block. Moreover, we can assign the data on the empty space of pilot signals for increasing the total transmission. In this paper, we propose an adaptive subcarrier block modulation with differentially modulated pilot symbol assistance for downlink OFDM using uplink delay spread.

*key words:* DMPSA-ASMS/OFDM, MLI, coherence bandwidth, RMS delay spread

## 1. Introduction

High data rate and high quality multimedia services are demanded in a fourth generation mobile communication, since application services are increasing. To meet this demand, orthogonal frequency division multiplexing (OFDM) is attractive and widely studied in recent years [1], [2]. Since the signals are transmitted in parallel by using many subcarriers that are mutually orthogonal and the corresponding spectrum is shaped like rectangle, OFDM can achieve high frequency efficiency and high data rate. Moreover, OFDM has been chosen for several next generation broadband WLAN standards like IEEE802.11a, IEEE802.11g and European HIPERLAN/2, and terrestrial digital audio broadcasting (DAB) and digital video broadcasting was also proposed for broadband wireless multiple access systems, such as IEEE802.16 wireless MAN standard and interactive DVB-T [3]–[5].

In general, each modulation scheme provides a trade off between spectral efficiency and the bit error rate (BER). Choosing the highest modulation scheme that will give an acceptable BER can maximize the spectral efficiency. Therefore, an adaptive modulation scheme (AMS) is one of efficient schemes to increase the throughput [6]–[11]. In an AMS/OFDM system, base station is in control of the modulation level of each subcarrier, and then, adaptive modulated packet is transmitted from the base station to the mobile station. In this case, the mobile station is required the modulation level information (MLI) to demodulate the received packet. The MLI is generally transmitted as a data symbol, therefore, the throughput is degraded in the downlink of AMS/OFDM due to the MLI transmission.

To reduce this problem, a fixed subcarrier block AMS/OFDM with variable coding rates has been proposed [12]. In this scheme, adjacent subcarriers are blocked to be assigned for the same modulation level with various coding rates for reducing the MLI transmission and the computational effort of the transmit power control. However, when the block size is large, the throughput might be degraded due to the mismatch between the block modulation level and the channel state and also many encoders and decoders are required. A differentially modulated pilot symbol assisted adaptive OFDM (DMPSA-AMS/OFDM) also has been proposed to reduce the MLI transmission [13], [14]. DMPSA-AMS/OFDM transmits the MLI as a differentially modulated pilot signal, so the total transmission rate is not degraded.

However, in fact, the channel response at a particular subcarrier frequency is not supposed to be totally different from its neighboring frequencies, and hence, they must have correlation which depends on the coherence bandwidth of the channel  $B_c$  [15]. Moreover, in frequency-division duplexing (FDD) systems, given the small frequency separation, the up-link and downlink channel share many common features, i.e., the number of paths, the path delays and the DOAs, which are the same for both links and are not frequency dependant [16], [17]. Thus, in FDD systems, the channel parameters that can be used at the base station for downlink adaptive modulated transmission are not the channel frequency response estimated on each subcarrier of the uplink but the information of the number of paths and path delays. The coherence bandwidth of the downlink is eas-

Manuscript received October 28, 2004.

Manuscript revised January 20, 2005.

Final manuscript received February 16, 2005.

<sup>†</sup>The authors are with The National Institute of Information and Communication Technology (NICT), Incorporated Administrative Agency, Yokosuka-shi, 239-0847 Japan.

<sup>††</sup>The author is with the Department of Information and Computer Science, Keio University, Yokohama-shi, 223-8522 Japan.

\*Presently, with the Department of Computer Engineering, Hiroshima City University, Japan.

a) E-mail: junny700@nict.go.jp

DOI: 10.1093/ietfec/e88-a.7.1889

ily calculated by using the uplink delay spread. If we could assign the same modulation level for coherently faded subcarrier block, MLI is required only one time for each subcarrier block. Since the data can be assigned and transmitted on the empty space of pilot signals, we can increase the total transmission rate. In this paper, we propose an adaptive subcarrier block modulation using uplink delay spread with differentially modulated pilot symbol assistance for downlink OFDM (DMPSA-ASMS/OFDM). This paper is organized as follows. The proposed DMPSA-ASMS/OFDM is described in Sect. 2, In Sect. 3, we show the simulation results. Finally, the conclusion is given in Sect. 4.

## 2. Proposed System

Figure 1 shows the proposed DMPSA-ASMS/OFDM. Here, we explain the adaptive subcarrier block modulation using uplink delay spread with differentially modulated pilot symbol assistance for downlink OFDM.

### 2.1 Coherence Bandwidth

In an OFDM, the channel response at a particular subcarrier frequency is not supposed to be totally different from its neighboring frequencies, and hence, they must have correlation which depends on the coherence bandwidth of the channel  $B_c$ . In FDD systems, the separation between uplink and downlink frequencies is about 5% of the mean frequency. Therefore, the instantaneous phase and amplitude

variation due to fading in the uplink have no correlation to those in the downlink. This means that the principle of reciprocity cannot be used. Fortunately, however, given the small frequency separation, the uplink and downlink channel still share many common features, i.e., the number of paths, the path delays, and the DOAs, which are the same for both links and are not frequency dependant [16], [17]. Thus, in FDD systems, the channel parameters that can be used at the base station for downlink adaptive modulated transmission are not the channel frequency response estimated on each subcarrier of the uplink but the information of the number of paths and path delays. In the base station, the channel informations such as the number of paths, the path delays can be obtained by using an IFFT operation of the frequency domain channel impulse response that estimated from the pilot signals. The transmitted pilot signals from the mobile station are already known, and each transmitted pilot signals value is assumed to be  $p_{i,t} = 1$ . The evaluated channel response includes the fading term, so we can compensate the amplitude and phase of the received signal.

$$\mathcal{H}_i = \sum_{t=1}^{N_p} \hat{p}_{i,t} / N_p, \quad (1)$$

where  $N_p$  is the number of pilot symbols,  $\mathcal{H}_i$  is the uplink channel impulse response on the  $i$ th subcarrier,  $\hat{p}_{i,t}$  is the received pilot signal on  $i$ th subcarrier and  $t$ th pilot symbol, respectively. To obtain an accurate channel impulse response, pilot symbol averaging is necessary to reduce the noise effect. In this paper, we consider two pilot symbol as an averaging duration for the channel tracking. Equation (1) shows the channel impulse response in the frequency domain. By using an IFFT operation and Eq. (1), the channel informations such as the number of paths, the path delays can be obtained. The path delays are calculated by using the channel impulse response. If the power density of uplink is discrete like Fig. 2, the root-mean-square (*rms*) delay spread of the transmission channel can be obtained as

$$\tau_{rms} = \sqrt{\tau^2 - (\tau_{av})^2}, \quad (2)$$

where  $\tau^2 = \sum_{n=1}^N |h_n|^2 \cdot \tau_n^2 / \sum_{n=1}^N |h_n|^2$ ,  $\tau_{av}$  is the average delay as  $\tau_{av} = \sum_{n=1}^N |h_n|^2 \cdot \tau_n / \sum_{n=1}^N |h_n|^2$ , and  $n$  is the index of each propagation path. The coherence bandwidth is inversely proportion to the *rms* delay spread. However, their exact relationship cannot be obtained since it usually depends on the fre-

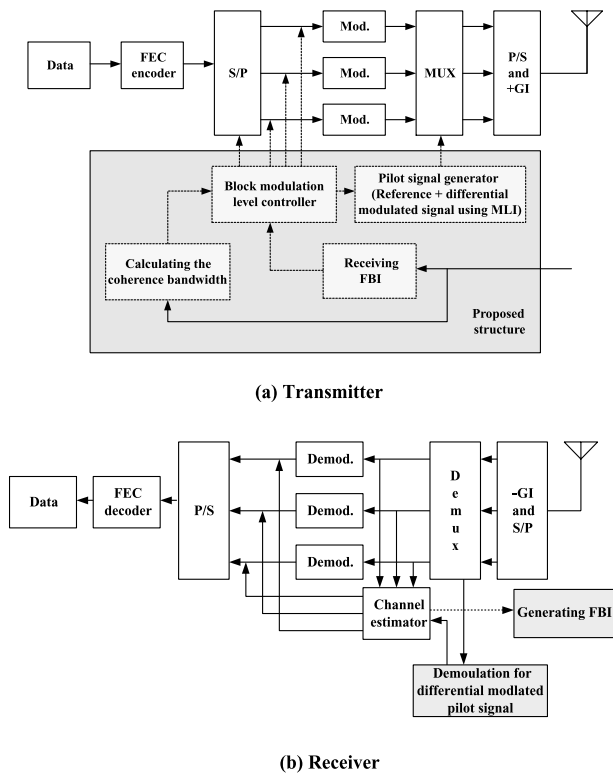


Fig. 1 Proposed system.

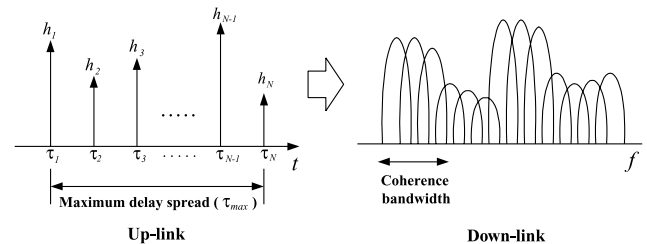


Fig. 2 The relation between uplink delay spread and downlink coherence bandwidth.

quency correlation function of time-varying multipath environments. A strict condition on the frequency correlation function as in [15] that leads the coherence bandwidth of  $B_c \approx \frac{1}{5 \cdot \tau_{rms}}$  is assumed in this paper. Consider an OFDM system with transmission bandwidth of 100 MHz, mean frequency is 5 GHz and 1024 subcarriers. The subcarrier bandwidth is  $\Delta f = \frac{100 \times 10^6}{1024} = 97$  kHz. Assume that the RMS delay spread ( $\tau_{rms}$ ) of mobile communication system is 500 ns, then the approximate coherence bandwidth is given by

$$B_c \approx \frac{1}{5 \cdot \tau_{rms}} = 0.4 \text{ MHz} \approx 4.12 \Delta f. \quad (3)$$

As a result, about 4 consecutive subcarriers are faded coherently. From Eqs. (2) and (3), we can easily calculate the coherence bandwidth for the downlink using the uplink channel delay spread.

## 2.2 MLI for Downlink Subcarrier Block Modulation

From Eq. (3), we can assign the same modulation level for coherently faded subcarrier block. In this case, the MLI is required only one time for each block. Thus, we can assign and transmit a more data on the empty space of pilot signals as shown in Fig. 3(b). Therefore, the proposed DMPSA-ASMS/OFDM can increase the total transmission rate to compare with the conventional DMPSA-AMS/OFDM. Now, we explain the MLI and data transmiss-

ion procedure on the pilot signals. We assume a Rayleigh frequency selective fading channel where the received signals are corrupted by additional noise and fading. We use complex baseband notation at time  $t$ , we transmit the  $i$ th subcarrier pilot signal  $p_{i,t}$ , and we receive the noisy  $i$ th subcarrier signal  $x_{i,t}$  at the receiver antenna. The received pilot signal is given by

$$x_{i,t} = h_{i,t} \cdot p_{i,t} + n_{i,t}, \quad t = 1, 2, \dots, N_p \quad (4)$$

where  $n_{i,t}$  is the additive noise which is the complex Gaussian zero-mean unit-variance distribution. The transmitted pilot signals are normalized to have power one when averaged out over time  $\mathbb{E}|p_{1,t}|^2 = 1$ . For a data rate of  $R$  bits per channel use, we need  $L = 2^R$  symbols. A common technique is PSK, which uses symbols that are  $L$ th roots of unity

$$v_l = e^{j2\pi l/L}, \quad l = 0, 1, \dots, L-1. \quad (5)$$

From Eq. (3), the number of coherence bandwidth subcarrier block and subcarrier in a subcarrier block are given by

$$N_{sb} = \lfloor B_w/B_c + 1 \rfloor \quad (6)$$

$$N_{coh} = \lfloor B_c/\Delta f \rfloor \quad (7)$$

where  $\lfloor x \rfloor$  stands for the integer lower and closer to  $x$ ,  $B_w$  is the transmission bandwidth of OFDM and  $\Delta f$  is a subcarrier bandwidth, respectively. Suppose we want to send MLI and data sequence of integers  $z_{i,1}, z_{i,2}, \dots, z_{i,N_p}$  with  $z \in \{0, 1, 2, \dots, L-1\}$  on the pilot signals. The transmitter sends the symbol stream  $p_{i,1}, p_{i,2}, \dots$  where

$$p_{i,t} = v_{z_{i,t}} p_{i,t-1}, \quad t = 1, 2, \dots, N_p \quad (p_{i,1} = 1) \quad (8)$$

where the initial pilot symbol does not carry any information, MLI is assigned on  $i_d$ th subcarrier of pilot where  $i_d$  is  $(n_{sb}-1)N_c+1$  with  $n_{sb} \in \{1, \dots, N_{sb}\}$  and data is assigned on  $i \neq i_d$ th subcarrier of pilot. If we assume that the fading coefficient changes slowly, the ML decoder is given by

$$\hat{z}_{i,t,ML} = \arg \min |x_{i,t} - v_l x_{i,t-1,i}|^2. \quad (9)$$

The above expression is equal to

$$|x_{i,t-1}|^2 + |x_{i,t-1}|^2 - 2|x_{i,t}x_{i,t-1}| \cos(\arg x_{i,t-1} - 2\pi l/L). \quad (10)$$

This expression is minimized by minimizing the argument of the cosine. Thus, the ML decoder can be computed as

$$\hat{z}_{i,t,ML} = \lfloor \arg(x_{i,t}/x_{i,t-1})L/2\pi \rfloor \quad (11)$$

where  $\lfloor x \rfloor$  stands for the integer closer to  $x$ . From Eq. (11), we can easily obtain the MLI ( $\hat{z}_{i_d,t,ML}$ ) for each subcarrier block and a more transmitted data ( $\hat{z}_{i \neq i_d,t,ML}$ ) using the differential demodulation for pilot signals. Now, we explain the increased transmission rate for our proposed scheme. Consider an OFDM system with the effective transmission rate  $\eta_e$ , the number of data symbols  $N_d$ , the number of pilot symbols  $N_p$ , the number of subcarriers  $N_c$ , and the number of carriers that included a block size information  $N_{bl}$ , the increased effective transmission rate  $\bar{\eta}_e$  is given by

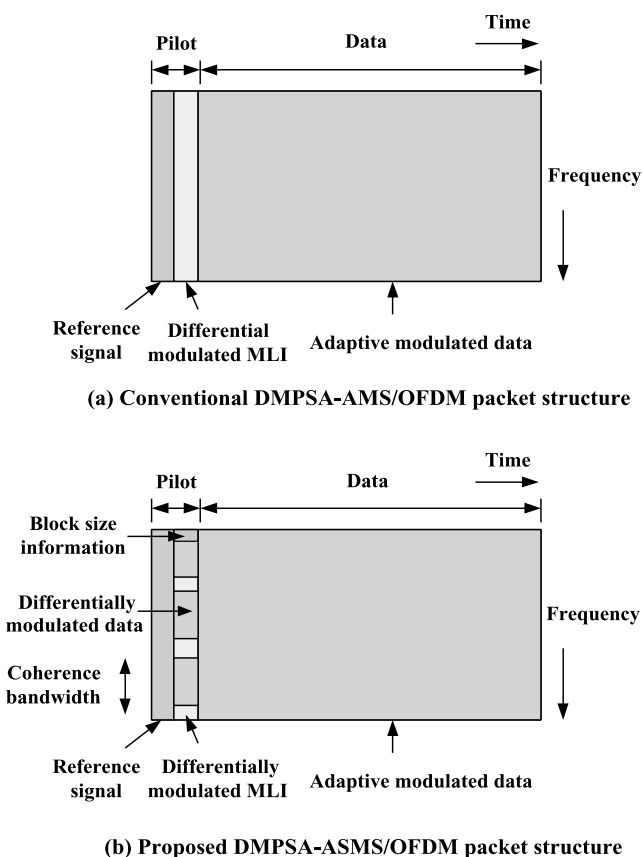


Fig. 3 The conventional and proposed packet structures.

$$\bar{\eta}_e = \eta_e + \hat{\eta}_e \cdot \frac{N_c - N_{sb} - N_{bl}}{N_c} \cdot N_p - 1 \quad (12)$$

where  $\hat{\eta}_e = \eta_e/N_d$  is the effective transmission rate for one data symbol. When the number of pilot symbol is small, the effect of transferring MLI bits on the empty pilot signals is small. As a result, the impact of MLI is small. On the other hand, when the number of pilot symbols is large, a more data can be transmitted on the pilot symbols. Moreover, the throughput depends on the delay spread. When the delay spread is large, the throughput is degraded due to the narrow coherence bandwidth.

### 2.3 Channel Estimation

The roles of pilot symbols are to calculate the channel response vector and to compensate the faded received packet. However, the proposed system is transmitted a more data and MLI on the pilot symbols as shown in Fig. 3, so the channel estimation procedure is different to compare with the conventional scheme. Here, we explain the channel estimation procedure. The first symbol of the transmitted pilot symbols of  $i$ th subcarrier  $p_{i,1}$  is already known, and its value is assumed to be  $p_{i,1} = 1$ . The received first pilot symbol of  $i$ th subcarrier  $x_{i,1}$  includes the channel response of each subcarrier and noise term as shown

$$x_{i,1} = h_{i,1} + n_{i,1}. \quad (13)$$

In low  $E_b/N_o$ , noise power is large, so it is difficult to compensate the received data packet accurately by using the first pilot symbol. Since noise term is random signal with zero mean, averaging of the pilot symbols can mitigate the noise term. However, the pilot symbols include the MLI and data that are unknown, therefore, we cannot averaging of the pilot symbols. To obtain the accurate channel response, we make replica pilot symbols  $\sum_{t=1}^{N_p} \tilde{p}_{t,i}$  where  $\sum_{t=2}^{N_p} \tilde{p}_{t,i,d}$ ,  $\sum_{t=2}^{N_p} \tilde{p}_{t,i,d}$  are the differentially modulated MLI and data using Eqs. (11), and  $\tilde{p}_{1,i} = 1$ . The channel response of  $i$ th subcarrier is given by

$$\hat{H}_i = \frac{\sum_{t=1}^{N_p} x_{t,i} / \tilde{p}_{t,i}}{N_p}. \quad (14)$$

Noise power on the  $i$ th subcarrier is a square of difference between the received pilot signals  $\sum_{t=1}^{N_p} x_{t,i}$  and the multiplication of the estimated channel response of  $i$ th subcarrier and the replica pilot symbols.

$$N_{0,i} = \left( \frac{\sum_{t=1}^{N_p} x_{t,i} - \hat{H}_i \cdot \tilde{p}_{t,i}}{N_p} \right)^2. \quad (15)$$

Finally, we can calculate the  $E_{s,i}/N_{0,i}$  on the  $i$ th subcarrier

$$\frac{E_{s,i}}{N_{0,i}} = \hat{H}_i^2 / N_{0,i}. \quad (16)$$

From Eqs. (14) and (16), we can compensate the received data packet and make a feedback information for next adaptive modulation.

### 3. Computer Simulated Results

Figure 1 shows the simulation model for an adaptive OFDM with  $N_c = 1024$  subcarriers. In the transmitter side, data stream is first encoded. Here, convolutional codes (rate  $R = 1/2$ , constraint length  $K = 7$ ) are used, which have turned out to be efficient for transmission of an OFDM signal over frequency selective fading channel. The coded bits are then mapped to the modulation symbols of  $N_c = 1024$  subcarriers by using adaptive subcarrier block modulation command (ASMC) that calculated by Eqs. (3) and (16). Pilot symbols are differentially modulated by using the MLI and data such as Eq. (8). The OFDM time signal is generated by an inverse FFT and is transmitted over the frequency selective and time variant radio channel after the cyclic extension has been inserted. The transmitted signals are subject to broadband channel propagation as shown in Fig. 4. In this model,  $L = 18$  path Rayleigh fadings have exponential shapes with path separation  $T_{path} = 30, 70$  and  $140$  nsec. These cases cause severe frequency selective fadings. The maximum Doppler frequency is assumed to be  $10$  Hz. In the receiver side, the received signals are serial to parallel converted and  $N_c$  parallel sequences are passed to a FFT operator, which converts the signal back to the frequency domain. The received pilot symbols are differentially demodulated, and then, the MLI and data can be obtained by Eq. (11). These frequency domain signals are coherently demodulated by Eq. (14). After demodulation, the binary data is decoded by the Viterbi soft decoding algorithm. The simulation parameters are listed in Table 1. Figure 5 shows

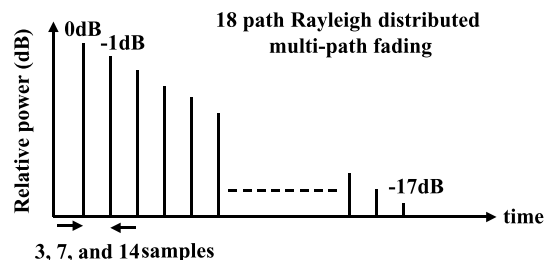


Fig. 4 Channel model.

Table 1 Simulation parameters.

Data modulation	QPSK,8PSK,16QAM
Pilot modulation	Differential QPSK
Data demodulation	Coherent detection
Pilot demodulation	Differential demodulation
Effect data rate	80 Msymbol/s
FFT size	1024
Number of carriers	1024
Guard interval	256 sample times
Frame size	12 symbols ( $N_p = 2, N_d = 10$ )
FEC	convolutional code ( $R=1/2, K=7$ )
Fading	18 path Rayleigh fading
Doppler frequency	10 Hz

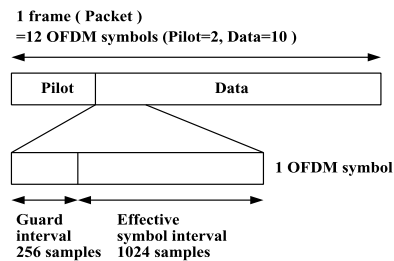


Fig. 5 Packet structure.

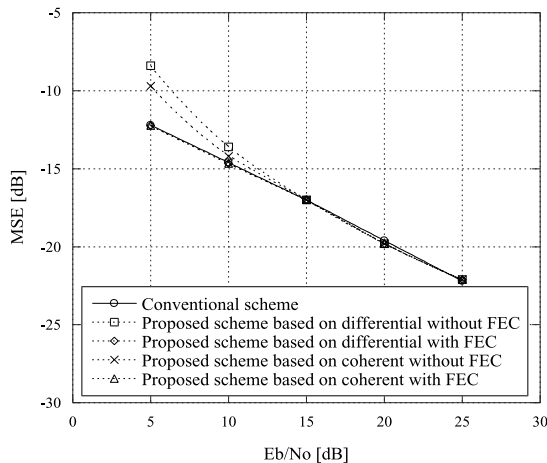


Fig. 6 MSE vs.  $E_b/N_0$  for conventional average pilot symbols channel estimation scheme and the proposed adaptive subcarrier block modulation with differentially modulated pilot symbol based scheme with and without FEC at Doppler frequency of 10 Hz.

packet structure. Packet consists of 1024 subcarriers and 12 OFDM symbols (number of pilot signals:  $N_p = 2$ , number of data:  $N_d = 10$ ). One OFDM symbol duration is  $12.8 \mu\text{sec}$ .

Figure 6 shows MSE vs.  $E_b/N_0$  for the conventional pilot symbol averaging channel estimation scheme and the proposed scheme with coherently and differentially modulated MLI and block size information on data symbols with and without a FEC at Doppler frequency of 10 Hz. The differential detection can easily demodulate a differentially modulated data without any channel information. On the other hand, the coherent detection is necessary an accurate channel information to compensate a faded data. In the proposed system, the received first pilot symbol of  $i$ th subcarrier  $x_{i,1}$  includes the channel response of each subcarrier and noise term as shown  $x_{i,1} = h_{i,1} + n_{i,1}$ . In low  $E_b/N_0$ , noise power is large, so it is difficult to compensate the received data packet accurately by using the first pilot symbol. Since the channel response is calculated from these demodulated MLI and block size information with errors, the proposed scheme with coherently and differentially modulated MLI and block size information on data symbols without a FEC shows worse MSE property than that of the conventional scheme. When we consider a FEC for the our proposed scheme, the channel estimation property is significantly increased. Therefore, the proposed channel estimation scheme

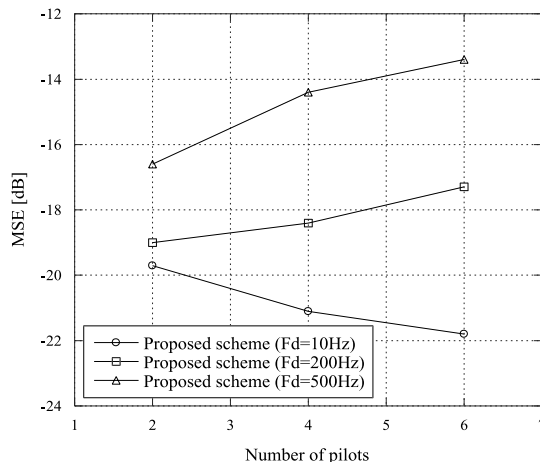


Fig. 7 MSE vs. number of pilots for the proposed schemes at  $E_b/N_0=20$  dB, and Doppler frequencies of 10, 200, and 500 Hz.

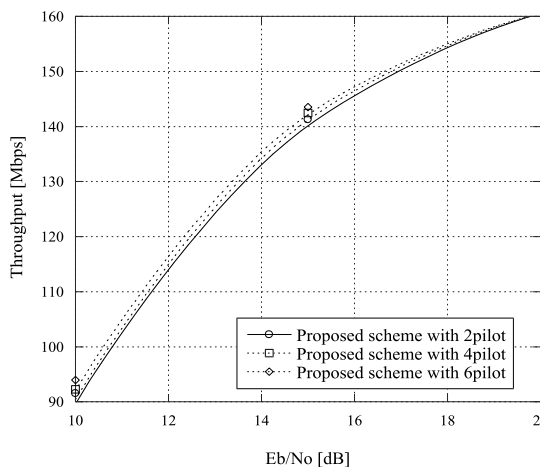
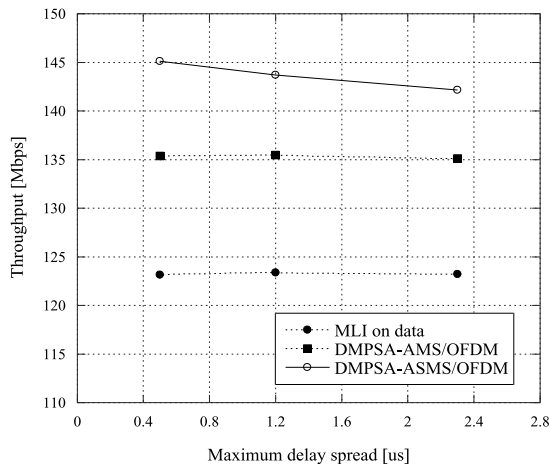


Fig. 8 Throughput of the proposed system for various number of pilots at Doppler frequency of 10 Hz and the maximum delay spread  $\tau_{max}=2.3 \mu\text{s}$ .

with a FEC shows the same property like the conventional scheme.

Figure 7 shows MSE vs. number of pilots for the proposed schemes at  $E_b/N_0=20$  dB, and Doppler frequencies of 10, 200, and 500 Hz. It is shown that the channel estimation property is increased with increasing the number of pilot symbols at Doppler frequency of 10 Hz. On the other hands, the channel estimation property is degraded with increasing the number of pilot symbols at Doppler frequency of 200 Hz and 500 Hz. This is because the channel varying is slow in low Doppler frequency, so the channel estimation property can be increased. However, in high Doppler frequency, channel is rapidly changed, so the channel estimation property is also degraded.

Figure 8 shows the throughput of the proposed system for various number of pilots at Doppler frequency of 10 Hz and  $\tau_{max}=2.3 \mu\text{s}$ . From Eq. (12), with increasing the pilot symbols, the total transmission rate would be increased. However, in this evaluation, the throughput of 4 and 6 pilot cases is not included an increased transmission rates that

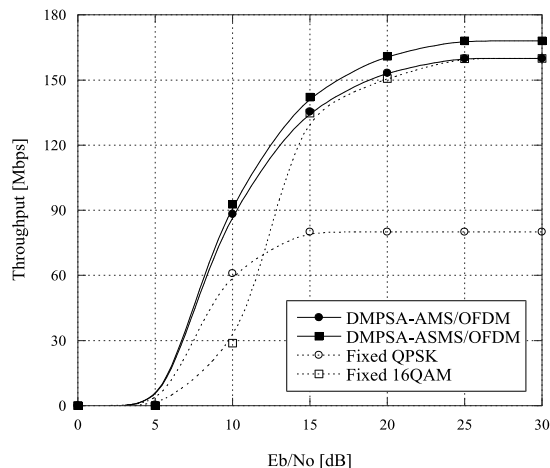


**Fig. 9** Throughput of various delay spreads on the performance of the conventional adaptive OFDM with MLI transmitting on data symbols, DMPSA-AMS/OFDM and DMPSA-ASMS/OFDM at  $E_b/N_0=15$  dB and Doppler frequency of 10 Hz.

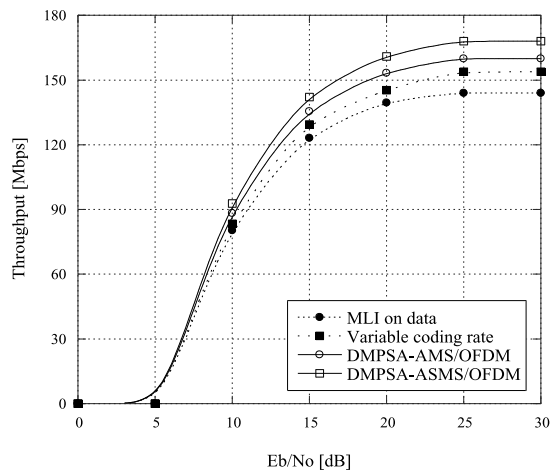
assign a data on the pilot empty space. The proposed system with 6 pilot symbols shows better throughput than those with 2 and 4 pilot symbols. Particularly, in low  $E_b/N_0$ , the proposed system with 6 pilot symbols shows large throughput gain to compare with high  $E_b/N_0$ . Since noise term is random signal with zero mean, averaging of the pilot symbols can mitigate the noise term. From this reason, the channel estimation property is increased with increasing the number of pilot symbols.

Figure 9 shows the throughput of various delay spreads on the performance of the conventional adaptive OFDM with MLI transmitting on data symbols, DMPSA-AMS/OFDM and DMPSA-ASMS/OFDM at  $E_b/N_0=15$  dB and Doppler frequency of 10 Hz. The conventional adaptive OFDM with MLI transmitting on data symbols and DMPSA-AMS/OFDM estimate the channel condition and assign the suitable modulation for each subcarrier. Therefore, the throughput of the conventional scheme and DMPSA-AMS/OFDM is the same with increasing the delay spread. However, the proposed scheme considers the coherence bandwidth and assigns a more data on the empty space of pilot signals. The coherence bandwidth is largely depended on the delay spread. With increasing the delay spread, the coherence bandwidth would be narrowed. Therefore, the total transmission of the proposed scheme is also degraded.

In Fig. 10, the throughput of fixed modulation schemes as QPSK and 16QAM, DMPSA-AMS/OFDM and proposed DMPSA-ASMA/OFDM are compared, where target BER of  $10^{-5}$ , Doppler frequency of 10 Hz and the maximum delay spread  $\tau_{max}=2.3 \mu s$ . Adaptive modulation schemes consist of QPSK, 8PSK, and 16QAM. It is shown that DMPSA-AMS/OFDM and DMPSA-ASMS/OFDM achieve better throughput performance than the fixed modulation schemes such as QPSK and 16QAM, since the channel capacity increases to allow the high level modulation



**Fig. 10** The throughput of fixed modulation schemes as QPSK and 16QAM, DMPSA-AMS/OFDM and the proposed DMPSA-ASMA/OFDM are compared, where target BER of  $10^{-5}$ , Doppler frequency of 10 Hz and the maximum delay spread  $\tau_{max}=2.3 \mu s$ .



**Fig. 11** The throughput of the conventional adaptive OFDM with MLI transmitting on data symbols, variable coding rate OFDM transmission, DMPSA-AMS/OFDM and the proposed DMPSA-ASMS/OFDM at Doppler frequency of 10 Hz and the maximum delay spread  $\tau_{max}=2.3 \mu s$ .

schemes like 8PSK and 16QAM in subcarriers with increasing  $E_b/N_0$ . Therefore, DMPSA-AMS/OFDM and DMPSA-ASMS/OFDM switch the channel modulation scheme from low-level modulation scheme as QPSK to high-level modulation schemes as 8PSK and 16QAM to increase the throughput performance. DMPSA-ASMS/OFDM can assign the same modulation level for coherently faded subcarrier block. In this case, MLI is required only one time for each subcarrier block. Thus the proposed scheme can assign and transmit the data on the empty space of pilot signals. Therefore, DMPSA-ASMS/OFDM can be obtained better throughput than that of DMPSA-AMS/OFDM.

Figure 11 shows the throughput of the conventional adaptive OFDM with MLI transmitting on data symbols, variable coding rate OFDM transmission, DMPSA-AMS/OFDM and the proposed DMPSA-ASMS/OFDM

at Doppler frequency of 10 Hz and the maximum delay spread  $\tau_{max}=2.3 \mu s$ . Since the conventional adaptive OFDM scheme transmits the MLI on data symbols, therefore, the total transmission rate is degraded. On the other hands, DMPSA-AMS/OFDM and DMPSA-ASMS/OFDM transmit the MLI on the pilot symbols with differential modulation. As a result, the total transmission rate is not degraded. Variable coding rate OFDM transmission shows worse throughput than those of DMPSA-AMS/OFDM and proposed DMPSA-ASMS/OFDM. In the variable coding rate based scheme, adjacent subcarriers are blocked to be assigned for the same modulation level with various coding rates for reducing the MLI transmission and the computational effort of the transmit power control. However, when the block size is large, the throughput might be degraded due to the mismatch between the block modulation level and the channel state. Therefore, the total transmission rate is degraded. The proposed DMPSA-ASMS/OFDM shows best throughput performance. The proposed DMPSA-ASMS/OFDM calculates the block modulation level using the coherence bandwidth to reduce the mismatch between the block modulation level and the channel state. From the simulated result, the proposed scheme obtains about 14%, 8% and 4% improvement to compare with the conventional scheme, variable coding rate based scheme and DMPSA-AMS/OFDM, respectively.

#### 4. Conclusion

In this paper, we proposed an adaptive subcarrier block modulation using uplink delay spread with differentially modulated pilot symbol assistance for downlink OFDM. The proposed scheme shows the same MSE performance like the conventional scheme. Moreover, the proposed scheme obtains about 14%, 8% and 4% throughput improvement to compare with the conventional scheme, variable coding rate based scheme and DMPSA-AMS/OFDM, respectively.

#### References

- [1] L. Cimini, "Analysis and simulation of a digital mobile channel using OFDM," *IEEE Trans. Commun.*, vol.33, no.7, pp.665–675, July 1985.
- [2] J.A.C. Bingham, "Multicarrier modulation for data transmission: An idea whose time has come," *IEEE Commun. Mag.*, vol.28, pp.5–14, May 1990.
- [3] ETSI ETS 301 958, "Digital video broadcasting (DVB); interaction channel for digital terrestrial television (RCT) incorporating multiple access OFDM," ETSI, Tech. Rep., March 2002.
- [4] "IEEE draft standard for local and metropolitan area network-part 16: Air interface for fixed broadband wireless access systems—Medium access control modifications and additional physical layer specifications for 2–11 GHz," *IEEE LAN MAN Standards Committee*, 2002.
- [5] I. Koffman and V. Roman, "Broadband wireless access solutions based on OFDM access in IEEE802.16," *IEEE Commun. Mag.*, vol.40, pp.96–103, April 2002.
- [6] R. Steele and W. Webb, "Variable rate QAM for data transmission over Rayleigh fading channel," *Proc. in wireless*, pp.1–14, Calgary, Albert, Canada, 1991.
- [7] T. Keller, T.H. Liew, and L. Hanzo, "Adaptive redundant residue number system coded multicarrier modulation," *IEEE J. Sel. Areas Commun.*, vol.18, no.11, pp.2292–2301, Nov. 2000.
- [8] T. Keller, T.H. Liew, and L. Hanzo, "Adaptive modulation techniques for duplex OFDM transmission," *IEEE Trans. Veh. Technol.*, vol.49, no.5, pp.1893–1904, Sept. 2000.
- [9] C. Wong, R. Cheng, K. Ben Lataief, and R. Murch, "Multiuser OFDM with adaptive subcarrier, bit, and power allocation," *IEEE J. Sel. Areas Commun.*, vol.17, no.10, pp.1747–1758, Oct. 1999.
- [10] H. Masuoka, S. Sampei, N. Morinaga, and Y. Kamio, "Adaptive modulation system with variable coding rate concatenated code for high quality multi-media communication systems," *Proc. VTC 1996*, pp.815–819, Piscataway, NJ, USA, 1996.
- [11] C. Ahn and I. Sasase, "The effects of modulation combination, target BER, Doppler frequency, and adaptive interval on the performance of adaptive OFDM in broadband mobile channel," *IEEE Trans. Consum. Electron.*, vol.48, no.1, pp.167–174, Feb. 2002.
- [12] T. Nakanishi, S. Sampei, and N. Morinaga, "Variable coding rate OFDM transmission on one-cell reuse TDMA systems," *IEICE Technical Report*, RCS2003-372, March 2004.
- [13] C. Ahn, S. Takahashi, and H. Harada, "Differential modulated pilot symbol assisted adaptive OFDM for reducing the MLI with predicted FBI," *IEICE Trans. Commun.*, vol.E88-B, no.2, pp.436–442, Feb. 2005.
- [14] C. Ahn, S. Takahashi, and H. Harada, "Differential modulated pilot symbol assisted adaptive OFDM for reducing the MLI," *IEICE Technical Report*, RCS2004-109, July 2004.
- [15] T.S. Rappaport, *Wireless Communication: Principle and Practice*, Prentice-Hall, 1996.
- [16] A.J. Paulraj and B. Chong Ng, "Space-time modems for wireless personal communications," *IEEE Pers. Commun.*, vol.5, pp.36–48, Feb. 1998.
- [17] G.G. Raleigh, S.N. Diggavi, V.K. Jones, and A. Paulraj, "A blind adaptive transmit antenna algorithm for wireless communications," *Proc. IEEE ICC'95*, vol.4, pp.1494–1499, June 1995.



**Chang-Jun Ahn** received the Ph.D. degree in the Department of Information and Computer Science in 2003 from Keio University, Japan. From 2001 to 2003, he was a research associate in the Department of Information and Computer Science, Keio University. In 2003, he joined the Communication Research Laboratory, Independent Administrative Institution (now the National Institute of Information and Communications Technology), Japan, as a researcher. His current research interests include OFDM, digital

communication, channel coding, and signal processing for telecommunications. Dr. Ahn received the ICF research grant award for Young Engineer in 2002 and the Funai Information Science Award for Young Scientist in 2003. He is listed in the Marquis Who's Who in Science and Engineering as a Telecommunication Engineer in 2004–2005 Edition. He is a member of IEE, IEICE, IEEE and the Korean Institute of Communication Science (KICS).



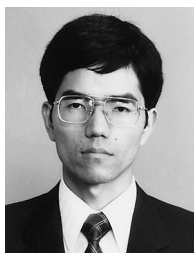
**Satoshi Takahashi** received B.E., M.E., and Ph.D., from Tokyo Denki University, Japan, in 1990, 1992, and 2002, respectively. From 1992, He joined Hitachi, Ltd., where he engaged in research on indoor radio propagation prediction and in the development of the radio communication systems. From 1996 to 1999, he has been a research engineer of the Communication System Department in YRP Key Technology Laboratories Co., Ltd., where he engaged in research on microwave mobile radio propagation. From

2002 to 2005, he has been a researcher in the Communication Research Laboratory (now the National Institute of Information and Communications Technology). From 2005, he is an Associate Professor in the Department of Computer Engineering, Hiroshima City University, Japan. Dr. Takahashi was an associate editor in IEICE Transactions on Communications. He received the Young Engineer Award of IEICE of Japan in 1999, the Young Engineer Award of IEEE-AP Japan chapter in 2000 and the telecommunications advancement foundation for Young Engineer Award in 2003. He is a member of the IEEE.



**Hiroshi Harada** received Ph.D. Degree from Osaka University, Osaka, Japan in 1995. From 1995, he joined the Communication Research Laboratory (now the National Institute of Information and Communications Technology), Ministry of Posts and Telecommunications (MPT), Tokyo, Japan. From 1996 to 1997, he was a postdoctoral fellow of Delft University of Technology, The Netherlands. He is currently a leader of wireless Access Group. His current research interests include digital-signal-

processing based mobile communication system, e.g. software radio and multimedia mobile access communication (MMAC) systems. Dr. Harada received the Young Engineer Award of IEICE of Japan in 1999 and the Excellent Paper Award of the Third WPMC in 2000. Dr. Harada is a member of the IEEE.



**Yukiyoichi Kamio** received the B.Sc., in humanities and science from Nihon University, Tokyo, Japan in 1981. In 1982, he joined the Radio Research Laboratory (now the National Institute of Information and Communications Technology), Ministry of Posts and Telecommunications, Japan, where he was engaged in developing error control coding, modulation and equalization techniques for land mobile communication systems. During 1999–2001, he was a Head of the Radio Transmission Department,

YRP Mobile Telecommunications Key Technology Research Laboratories Co., Ltd. From 2002, he is working in the National Institute of Information and Communications Technology, Independent Administrative Institution, Japan as a senior researcher. Mr. Kamio is an Editor of IEICE Transactions on Communications. He is a member of the IEEE.



**Iwao Sasase** received the B.E., M.E., and Ph.D. degrees in electrical engineering from Keio University, Yokohama, Japan, in 1979, 1981 and 1984, respectively. From 1984 to 1986, he was a Post Doctoral Fellow and Lecturer of Electrical Engineering at the University of Ottawa, ON, Canada. He is currently a Professor of Information and Computer Science at Keio University, Yokohama, Japan. His research interests include modulation and coding, mobile and wireless communications, optical commu-

nications, communication networks, and information theory. He has authored over 220 journal papers and 314 international conference papers. Dr. Sasase received the 1984 IEEE Communications Society (ComSoc) Student Paper Award (Region 10), 1986 Inoue Memorial Young Engineer Award, 1988 Hiroshi Ando Memorial Young Engineer Award, 1988 Shinohara Memorial Young Investigators Award, and 1996 IEICE Switching System Technical Group Best Paper Award. He serves as the Director of IEEE ComSoc Asia Pacific Board, the Chair of IEICE Network Systems Technical Group, and the Chair of Photonic Internet Forum Planning Committee, etc. He is a senior member of IEEE, and a member of the Information Processing Society of Japan (IPSI) and SITA of Japan.